Polímeros
ISSN 1678-5169 (Online)

https://doi.org/ 10.1590/0104-1428.20250060

ORIGINAL ARTICLE

Enhanced thermal and transport properties of PP/$CaCO_3$ micro- and nanocomposites: performance evaluation

Juliano Martins Barbosa[1,2]*, Renato Meneghetti Peres[1], Bruno Milton Oliveira Silva[1], Ricardo Jorge Espanhol Andrade[1,3] and Hélio Ribeiro[1]

[1]Engenharia de Materiais, Escola de Engenharia, Universidade Presbiteriana Mackenzie, São Paulo, SP, Brasil
[2]Programa de Pós-graduação em Ciência e Engenharia de Materiais – PPGCEM, Departamento de Engenharia de Materiais – DEMa, Universidade Federal de São Carlos – UFSCar, São Carlos, SP, Brasil
[3]Instituto Mackenzie de Pesquisa em Grafeno e Nanotecnologias – MackGraphe, Universidade Presbiteriana Mackenzie, São Paulo, SP, Brasil

**barbosa_jm@yahoo.com.br*

Abstract

Mechanical tests previously demonstrated that optimizing the dispersion of micro- and nanoparticulate $CaCO_3$ in polypropylene (PP) composites was successfully achieved through a Design of Experiments (DOE), enabling the identification and guided processing parameters for further evaluation of thermal and barrier properties. The formulation with 1.2 wt% nanofiller exhibited enhanced crystallinity compared to hPP. The incorporation of ~4.0 wt% nanoparticulate $CaCO_3$ increased the Heat Deflection Temperature (HDT) by 12 °C compared to neat homopolymer polypropylene (hPP), and by 3 °C relative to microfilled composites. Oxidation Onset Temperature (OOT) improved with increasing filler content, especially in nanocomposites. A slight reduction in flammability was observed for the composite with ~0.5 wt% nanofiller. Water Vapor Transmission Rate (WVTR) remained mostly unchanged in microcomposites, while a 1.5 wt% microfilled sample showed excellent Oxygen Transmission Rate (OTR) performance. Notably, nanocomposites containing 0.48wt% $CaCO_3$ reduced OTR by 52%, confirming their thermal stability and barrier properties at low filler loadings.

Keywords: *calcium carbonate, polypropylene nanocomposites, barrier properties, oxygen transmission rate (OTR), water vapor transmission rate (WVTR).*

Data Availability: All data supporting the findings of this study are available at UFSCar Institutional Repository – https://repositorio.ufscar.br/handle/ufscar/15929.

How to cite: Barbosa, J. M., Peres, R. M., Silva, B. M. O., Andrade, R. J. E., & Ribeiro, H. (2026). Enhanced thermal and transport properties of PP/$CaCO_3$ micro- and nanocomposites: performance evaluation. *Polímeros: Ciência e Tecnologia*, *36*(1), e20260008. https://doi.org/10.1590/0104-1428.20250060

1. Introduction

Mineral fillers are considered solid, inorganic, insoluble additives that, when incorporated into polymers, can reduce the cost of the product or enhance its mechanical, thermal and transport properties[1]. $CaCO_3$ is the most widely used in plastics due to its low cost and abrasiveness, good dispersion, food contact approval and low refractive index[2], classified as natural or precipitated[3] and can be used in micro and nanocomposites via techniques like: vapor deposition, reactive precipitation, sol-gel, and microemulsion, with simplicity, low cost, and scalability[4]. High-Gravity Reactive Precipitation (HGRP) is also a key technology for producing nano particles of $CaCO_3$, driving interest in polymer nanocomposites for their superior properties over microcomposites that contain larger particles[5-7], enhance performance, enabling unique chemical and physical interactions and properties[8-10]. The PP/$CaCO_3$ nanocomposite can be processed by *in-situ* polymerization, melt blending, and sol–gel processes, each with their own specific advantages and disadvantages[11,12]. These composites are generally used to enhanced their physical and chemical properties[13], such as barrier, flame retardant, thermal and mechanical resistance[14,15]. Nanocomposites, based on nanoclay, for instance, form organic-inorganic hybrids by intercalating polymer chains between exfoliated clay layers, creating nanometric multilayers. Other fillers, like $CaCO_3$, silica, talc, mica, carbon black, among others, are also used[7,9,10,16]. In this context, an efficient dispersion of nanoparticles can be achieved through surface modification, the use of dispersant and compatibilizer agents, whereas extrusion blending provides a practical engineering route[11,12]. Through DSC analysis, it was possible to demonstrate that nano-$CaCO_3$ with acrylic acid increases PP crystallization temperature via efficient nucleation[14]. Mechanical tests revealed that nano-$CaCO_3$ outperforms micro-$CaCO_3$, reinforcing and stiffening PP, forming smaller and imperfect spherulites that induces the β-phase of PP[17], which can slightly improve tensile strength, but gradually reduces elasticity at higher concentrations. The addition of 1.5 wt% of the non-ionic modifier significantly increased the impact resistance, without affecting the tensile strength or elastic

modulus[12,18,19]. Barbosa et al.[5,20,21] studied mechanical, thermal, and flammability properties of PP/$CaCO_3$ composites with different wt% of nano and micro filler in which it was shown that nano-$CaCO_3$ improved impact resistance and HDT in relation to the pure polymer and the microcomposite. Flammability tests showed a slight reduction in burn rate compared to pure PP, indicating that $CaCO_3$ enhances flame resistance by forming a protective layer during combustion that limits fire spread[5,20,21]. Alves et al.[22] investigated the flammability of PP nanocomposites (organophilic clay), found that adding 5wt% clay decreased the burn rate compared to pure PP, indicating formation of protective barriers, reducing fire propagation. In another work[23], PP/$CaCO_3$ composites (30wt%) with poly(ethylene-co-vinyl acetate) showed a thermal stability increase of up to ~33 °C, indicating improved oxidation resistance, however, a 15 °C reduction in HDT[23]. Hadi et al.[24], valuated the effect of $CaCO_3$ nanoparticles on thermoplastics and found that their addition improved UV resistance, associated with greater oxidation stability and better performance under harsh environmental conditions. Loste et al.[25] reviewed the growing demand for advanced functional materials, emphasizing transparent nanocomposites and their barrier properties, particularly how nanoparticles improve resistance to gas and vapor permeation in packaging applications. Al-Samhan and Al-Attar[26] investigated the impact of micro and nanoparticulate $CaCO_3$ on the mechanical, thermal and barrier properties of PP composites, finding that the nano enhanced thermomechanical properties, increased *Tg* by up to 30 °C, raised crystallization temperature by 14% and reduced Water Vapor Permeability (WVTR) to just above 7.0 g/m^2 by 24 h, indicating properties improvement. Kamal et al.[27], determined that PP´s HDT increased with the addition of treated nano $CaCO_3$, compared to untreated nanocomposites. In this context, it was observed that, to date, no comprehensive study about barriers and transport properties of these PP-based micro and nanocomposites has not been investigated yet. From our previous works[5,20,21], it was investigated the influence of micro and nano $CaCO_3$ particles in the PP matrix in their thermal and mechanical properties.

2. Materials and Methods

The used nanoparticulates precipitated $CaCO_3$ NPCC-201 (D_{50}: 40 nm, SSA: 40 m^2/g, purity >94.5%) from NanoMaterial Technology Pte Ltd – Singapore[5], microparticulate $CaCO_3$ Omyacarb 1T-AV (D_{50}: 1.6–1.7 µm, purity >97.3%) from Omya International AG – Italy[5], compatibilizer PP-g-MA Fusabond P MD353D (MFI: 450 g/10 min – 2.16 kg @ 190 °C, MP: 136 °C, >1.0% MA), from DOW Inc[5] and hPP H301 (MFI: 10 g/10 min) supplied by Braskem S.A[5]. The study unfolded in two phases: First involved Designing of Experiments (DOE), combined three variables at two levels: Extruder screw rotation (N: 250 and 500 rpm), Extruder feed flow (Q: 10 and 15 kg/h) and D_{50} (ϕ: 40nm and 1.7mm), to prepare and dilute the concentrates[5,20,21]. The formulations and their processing conditions were reported in Table 1 of Barbosa et al.[21]. Overall, a concentrate was produced using a co-rotational twin-screw extruder, adjusting shear levels via SME and varying extrusion parameters (N and Q), in the sequence, dilutions of the concentrates were then made to produce micro and nanocomposites, which were characterized as mechanical, thermal, and transportation properties. The processing parameters were defined with a 500 rpm (N) and 10 kg/h (Q) yield the best performance. Thermal and transport properties were tested with PP/$CaCO_3$ microparticles (M_500_10) and nanoparticles (N_500_10) composites. The indices 500 represent the rotation speed (rpm), and 10 refers to the Q value employed to evaluate the effect of these fillers regarding their content and particle size (ϕ). These samples were compared with pure hPP (B_500_10), processed at same conditions. The second part of our previous work focused on the characterization, including the structural and morphological properties of the $CaCO_3$ particles, their size distributions, and the morphology and mechanical properties of the micro- and nanocomposites, as reported Barbosa et al.[5,21].

2.1 Characterization

Firstly, it was identified the process conditions that ensured superior filler dispersion and improved tensile and impact strength properties in the nanocomposite compared to the microcomposite and/or hPP, as well as a lower nanoparticle activation volume at the same concentration[21] As described in Barbosa et al.[21], the morphological characterization of $CaCO_3$ particles was carried out by SEM using a Zeiss-Supra 35 microscopes. The average particle sizes of $CaCO_3$ micro- and nanoparticles were determined through ImageJ software analysis. X-ray Diffraction (XRD) patterns were obtained with a Rigaku DMax 2500 PC diffractometer (Cu Kα radiation, λ = 1.54056 Å) over a 2θ range from 5° to 75°. The specific surface area (BET) measured using a Micromeritics ASAP 2000 V3.03 A (N_2 atmosphere). The study progressed to evaluate others complementary properties, such as the Thermal (HDT, Flammability and OOT) and Transport properties (WVTR and OTR) under these parameters, considering the influence of filler content and particle size (ϕ). The composites exhibit thermal properties of interest, which can be determined using techniques such as HDT (Heat Deflection Temperature), OOT (Onset Oxidation Temperature) and Flammability testing. For these tests, the specimens were molded by injection mold, using a Pavan Zannete NFN 150P machine at 200 °C and 70 bar injection pressure, with a mold temperature of 23 ± 2 °C. The HDT test was conducted following ASTM D648 standards[28] (455 kPa, 100 mm support span, T_0: 26 °C and heating rate of 120 °C/h) and specimens with 12.95 x 3.00 mm. The OOT test was performed following ASTM E2009[29], using a thermal analyzer DSC 300 *Caliris Classic* (heating rate of 10 °C/min and 50 mL/min of O_2). Finally, the flammability test was conducted in accordance with UL 94 - HB[30] classification (L: 125 ± 5, W: 13 ± 0.5 and t: 1.6 ± 0.2 mm), and the specimen must not burn at a speed greater than 40 mm/min over a span of 75 mm.

2.2 Barrier or transport properties

The specimens, in film form (t = 40-100 µm), were prepared using a hot press (T_m = 180 °C @ 3000 psi for 3 min). Afterward, the heating system was turned off, and the cooling system was activated while maintaining pressure until room temperature was reached [31].

2.2.1 Water vapor transmission rate (WVTR)

Using gravimetric method with exposure to water vapor (polar environment)[32]. The Flow (J) was determined by the mass variation over time, corrected by the exposed film area (where Δm = mass variation, Δt = time variation and A = exposed test area), as shown in the Equation 1. The value of Δm/Δt was obtained from the slope of the line (tanα) generated in the steady state.

$$J = \frac{m}{t} \times \frac{1}{A} \quad (1)$$

By applying *Fick's First Law*, which establishes the proportionality between the Material Flow and the concentration gradient, the water vapor transition permeability coefficient (P_w) can be determined, as shown in Equation 2, where: ΔP_v = vapor pressure variation, L = polymer film thickness, P_v^{ext} = vapor pressure outside the system and P_v^{int} = vapor pressure inside the cup.

$$J_w = \frac{-P_w \Delta P_v}{L} = \frac{P_w\left(P_v^{ext} - P_v^{int}\right)}{L} \quad (2)$$

By correlating *Fick's First Law* and the *Steady-State Theory*, the relationship between Flow (J) and Permeability (P_w) is obtained, as given in Equation 3[33].

$$P_w = \frac{J \times L}{\Delta P_v(T)} = \frac{J \times L}{c} \quad (3)$$

The test was conducted at T = 30 °C (303 K), with the tabulated value for ΔPv = 31.8 mmHg. For better clarity in this equation, ΔPv was replaced with concentration (c), calculated using the ideal gas equation, as shown in Equation 4, where P = pressure = ΔPv (30 °C) = 31.8 mmHg, R = ideal gas constant = 63.32×10^3 mmHg·cm^3·mol^{-1}·K^{-1} and T = test temperature = 303 K. By substituting the values into Equation 4 and multiplying by the molar mass of water, we obtain c = 3,024x10^{-5} g.cm^{-3} and the Permeability (Pw) can be expressed in cm^2.s^{-1}

$$P = \frac{n \times R \times T}{V} = c \times R \times T \quad (4)$$

The films were cut to a 20 mm diameter and tested in triplicate using a Payne Cup apparatus, fixed at the top of the cup, with distilled water placed inside the cup[32,33]. The set is placed inside a sealed chamber called an isopiestic chamber (constant relative humidity). Within the chamber, a desiccant agent (P_2O_5) creates a pressure gradient, allowing water vapor to permeate through the polymeric film. The cups are initially weighed every 2 h and subsequently every 12 or 24 h. Thus, the mass variation (Δm), representing the amount of water permeated through the film, is determined by weighing the set.

2.2.2 Oxygen barrier properties (OTR)

Based on the partition method, where constant gas pressure is applied to one side of the membrane. The permeating gas diffuses through the membrane toward the opposite side, which has been initially evacuated[31], following ASTM D3985[34]. The pressure variation (ΔP) is measured over time (Δt), and the permeability value is automatically provided in the unit ccmil·m^2·day^{-1}, where 1 mil equals 1x10^{-3} inches or 2.4x10^{-3} cm. Conversion to cm^2·s^{-1} can be achieved by multiplying the obtained value by 2.78x10^{-12} and the test was conducted using the OX-TRAN model 2/21 from Mocon (23 °C@691.33 mmHg, cycles: 30 min, cell conditioning: 2 h and carrier gas: N_2/H_2)[34]. All analytical equipment employed in this study was located and operated in the state of São Paulo, Brazil.

3. Results and Discussions

SEM micrographs of $CaCO_3$ micro and nanoparticles are available in Barbosa et al.[5,20,21]. Briefly, the microparticles are in the form of flakes with an average size of ~1.5 μm, while the nanoparticles are spherical with sizes up to ~70 nm. Regarding X-ray diffraction (XDR), both the micro and nanoparticle samples presented characteristics diffraction patterns, expected for crystalline materials based on $CaCO_3$. The specific surface area of $CaCO_3$ particles, the nanoparticles presented a value of 24.19 ± 0.18 m^2/g, while the microparticles had a value of 6.89 ± 0.16 m^2/g. As previously reported by Barbosa et al.[5,20,21], the samples B_500_10, M_500_10 and N_500_10 composites were studied by SEM after cryogenic fracture to evaluate their particles dispersion and morphology. Figure 1 shows images with different magnifications of samples. Although $CaCO_3$ nanoparticles demonstrated better dispersion in hPP compared to microparticles, both particle sizes exhibited good distribution within the hPP matrix, as also observed by Mai et al.[4] and Yang et al.[11].

The XRD tests were conducted on B_500_10 and the micro and nanocomposites, as well as applied to the concentrates, detailed in the literature[5,20,21] and the results are presented in Figure 2. Sample 500_10, which contains different concentrations of the compatibilizing agent (grafted maleic anhydride), showed significant increases in the degree of crystallinity in all formulations. The crystallinity degree of hPP was ~66%, but with the addition of mineral fillers or compatibilizing agent, this value increased for lower concentrations. However, a progressive reduction of crystallinity was observed with an increase of the wt% compatibilizer. The same behavior was observed for the micro and nanocomposites, this decrease was more pronounced for nanocomposites from 5wt% of these nanostructures.

This effect can be due to interference in the nucleation and crystal growth mechanism caused by the higher wt% of mineral filler, which generates more aggregates, as observed in the concentrates M_500_10[5,20,21]. As the crystallization process is very sensitive to any material inserted in the host system, the reduction in crystallinity can be associated with the finer dispersion of nanoparticles. Moreover, this phenomena may interfere with the regular packing and alignment of polymer chains necessary for crystallite nucleation and growth, in contrast to the effects observed with microscale filler, as presented by Sakahara et al.[17]. In relation to the composites, low wt% of nanofiller exhibited high crystallinity (~71%), likely due to the good distribution of the nanoadditives in the polymer matrix, without disturbing the nucleation process. The incorporation of microparticles resulted in a slight increase in crystallinity compared to neat

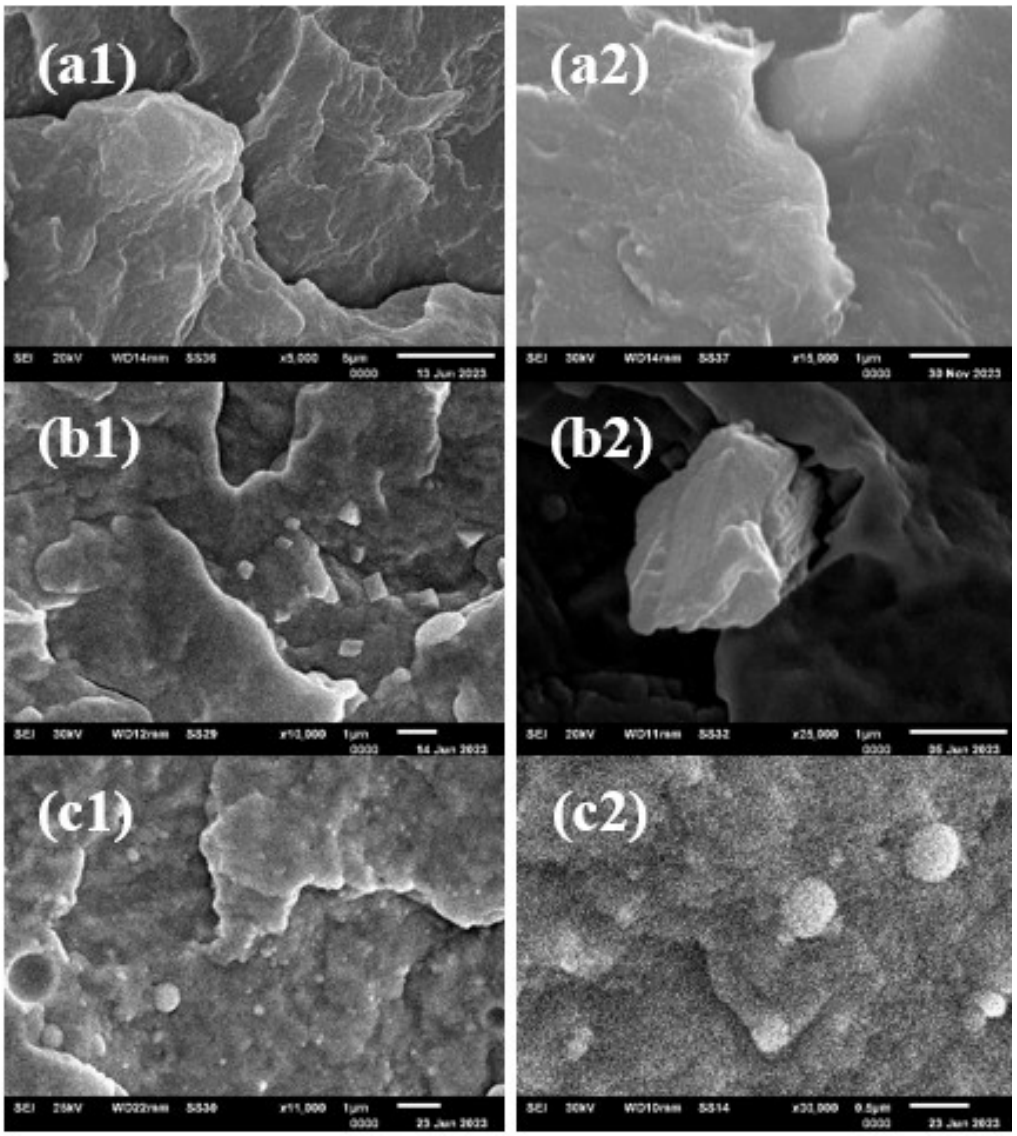

Figure 1. Micrographs of samples: hPP (B_500_10) - magnification of 5,000x (a1) and 15,000x (a2); M_500_10 – magnification of 10,000x (b1) and 25,000x (b2); N_500_10 – magnification of 11,000x (c1) and 30,000x (c2).

hPP; however, this increase was lower than that observed for the nanocomposites up to approximately 5 wt%. Beyond this concentration, the effect of filler content appears to become dominant, leading to a reduction in crystallinity in both micro- and nanocomposite systems. These results are consistent with the literature[35], although they are higher than those obtained by Chan et al.[36] and Eiras[37].

HDT measurements provide valuable insights into how the incorporation of mineral fillers can improve the structural rigidity and thermal endurance of polymers, supporting their application in thermally demanding environments. The incorporation of fillers led to a measurable increase in HDT across all formulations. Notably, the nanocomposite N_500_10 (5 wt%) exhibited the highest thermal deflection performance, reaching temperatures 12 °C above neat hPP and ~3 °C above its microparticulate counterpart, as shown in Figure 3. The results clearly showed that the addition of

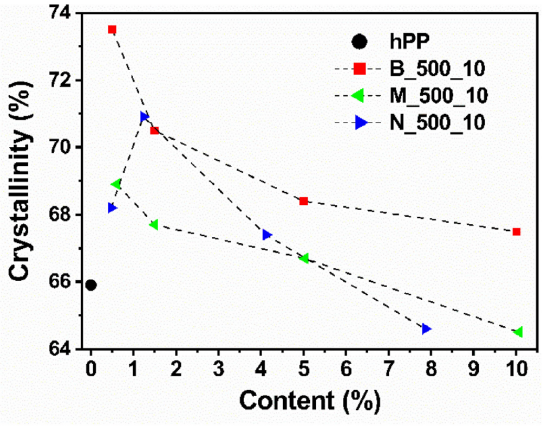

Figure 2. Crystallinity Degree of composites as a function of filler content.

nanoparticles was much more efficient in HDT than micro additives, probably due to greater dispersion and interaction with the polymer matrix[35].

Oxidation Onset Temperature (OOT) is a fundamental parameter for characterizing the thermal-oxidative stability of polymers. It defines the temperature at which noticeable oxidative degradation begins, and it is commonly determined using Differential Scanning Calorimetry (DSC). This technique is widely used to assess the performance of antioxidants, forecast material behavior under service conditions, and support the design of more stable and long-lasting polymeric formulations. Figure 4 presents the OOT results obtained for hPP, which exhibited an onset oxidation temperature of 223 °C. In comparison, the B_500_10 sample remained stable at approximately 225 °C, regardless of the compatibilizer concentration. In both composite systems, the OOT values exhibited a gradual decrease with increasing filler content; however, this reduction was more pronounced in the nanocomposite (N_500_10) than in the microcomposite (M_500_10). A review of the available literature revealed a lack of specific studies addressing the influence of $CaCO_3$ on the oxidation onset temperature (OOT) of hPP. Bertini et al.[38] investigated PP nanocomposites containing organophilic montmorillonite (OMMT) and reported that metal ions present in the clay can catalyze oxidative degradation, resulting in a decreased oxidation onset temperature (OOT). Similarly, Fitaroni et al.[39] observed that although thermogravimetric analysis demonstrated enhanced thermal decomposition temperatures with increasing filler content, the Oxidation Induction Time (OIT) measurements indicated a reduction in oxidative stability[38,39]. Regardless, in our case it was observed that both $CaCO_3$ micro and nano additives reduced the thermal stability of the polymer, and this effect was more pronounced at high values of wt% of load, considering the more pronounced effect of concentration for this property.

Additionally, the slope of the tangent line-representing the relationship between heat flow (dQ) and temperature (dT)- indicates the intensity of oxidation propagation. A steeper slope reflects a more vigorous exothermic reaction, as illustrated in Figure 5, which presents the thermal behavior of the composites[5,20,21]. The dQ/dT parameter reflects the oxidation kinetics in polymer composites, being influenced by the filler concentration and particle size. Nanoparticles presented higher dQ/dT and shorter thermal exposure time (OOT), while microparticles were more thermally stable. As shown, the heat flux increased with the addition of filler and is generally higher for nanoparticles. The best performance was observed for the microparticle composite with 1.5 wt% $CaCO_3$, while the nanoparticle composite with 1.2 wt% was more stable.

The flammability test assesses the fire resistance of polymeric materials, playing a crucial role in ensuring safety, regulatory compliance, and minimizing fire-related risks. It also guides the development of flame-retardant formulations and the selection of appropriate materials for applications where the protection of life and property is essential. According to UL94 classification, all samples were designated as Horizontal Burning (HB). The results indicate that neither particle size nor filler content had a significant effect on the burning rate, although a subtle trend was observed. The hPP exhibited the highest burning rate, while B_500_10 showed a slight reduction, likely attributable to the presence of the compatibilizer. The lowest burning rates were observed in the N_500_10_0.50 composite at low filler content. As illustrated in Figure 6, the addition of the compatibilizing agent along with micro- and nanoparticulate $CaCO_3$ effectively reduced the flammability of composites, as expected[23].

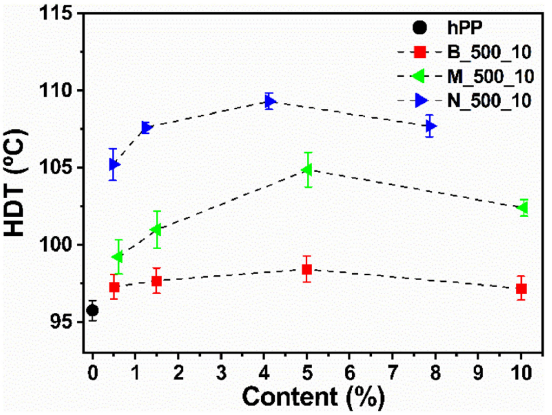

Figure 3. HDT results for the samples M_500_10 and N_500_10.

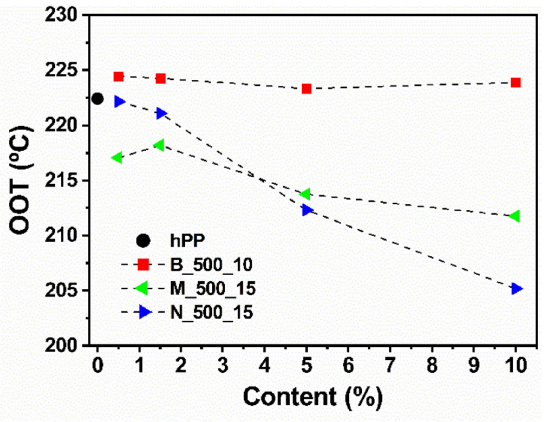

Figure 4. OOT of the hPP, B_500_10 and micro and nanoparticulate composites.

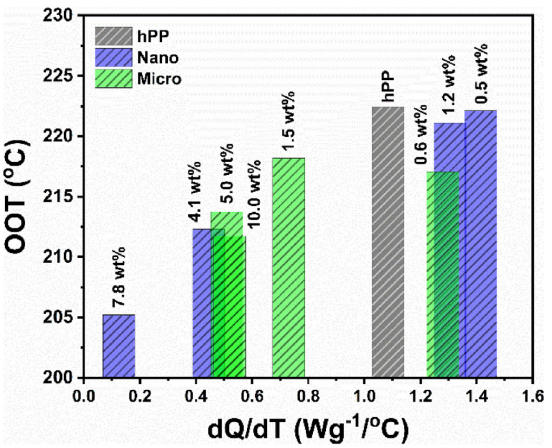

Figure 5. Heat flow of hPP and composites by temperature.

The Water Vapor Transmission Rate (WVTR) is a crucial measure of a polymer film's moisture barrier performance, vital for applications like food packaging, pharmaceuticals, and electronics. Accurate WVTR evaluation guides material selection, ensures regulatory compliance, and supports the development of advanced films with enhanced protective properties, expanding their industrial applicability. As shown in Figure 7, most composites and the compatibilized polymer exhibited increased WVTR values compared to neat hPP. In contrast, a significant reduction in permeability was observed for the N_500_10 composite at 1.5 wt% and the M_500_10 composite at 10 wt%, indicating enhanced barrier performance in these formulations. Although nanofillers are typically associated with improved barrier properties due to their high surface area and ability to create tortuous diffusion paths, the superior performance observed also in composites filled with microparticles at higher concentrations can be attributed to more uniform dispersion and reduced agglomeration. At elevated loadings, microparticles effectively occupy the free volume within the polymer matrix, limiting the mobility of water molecules and reducing permeability. Conversely, poorly dispersed or excessive nanoparticles may form agglomerates and defects, compromise the expected tortuosity and facilitate vapor transport. Therefore, barrier performance depends not only on particle size but also on dispersion quality, filler distribution, and concentration[17,26].

The Oxygen Transmission Rate (OTR) is essential for evaluating polymer films against small molecules, ensuring the protection of oxygen-sensitive products, compliance with standards, and the development of materials with enhanced barrier properties for diverse applications. In this case, the B_500_10 sample showed values comparable to those of hPP, indicating that the compatibilizer concentration had no significant effect on this property. As shown in Figure 8, nearly all composites exhibited higher oxygen permeability than the polymer matrix. Although nanoparticulate composites show a slight decrease in permeability at 1.5 wt%, the overlapping error bars prevent drawing a definitive conclusion. Regarding oxygen permeability, a correlation with the degree of crystallinity is evident: permeability increases as crystallinity decreases, and this variation is dependent on the $CaCO_3$ content[17,25].

Figure 9 presents the correlation between WVTR and OTR values of the samples. The degree of crystallinity may significantly influence the permeability of polymer composites, as higher crystallinity tends to reduce permeability by creating a denser, more ordered structure that limits gas and vapor diffusion. Mineral fillers may act as nucleating

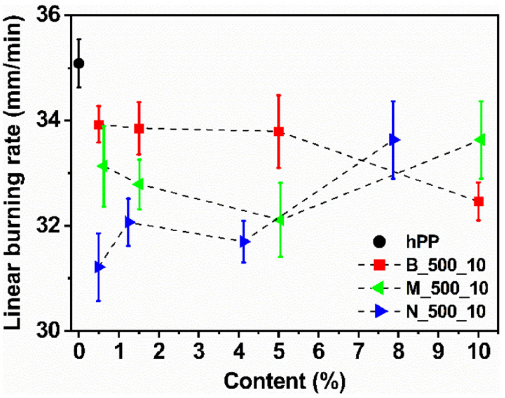

Figure 6. Linear burning rate of composites.

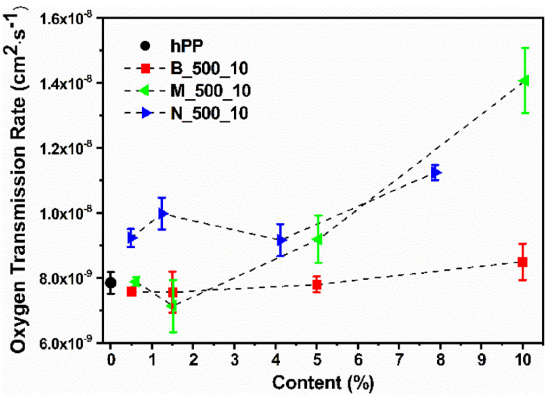

Figure 8. Oxygen Transmission Rate (OTR) for composites.

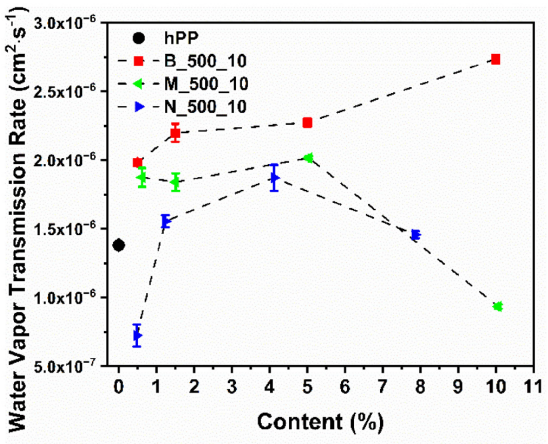

Figure 7. Water vapor transmission rate (WVTR) for composites.

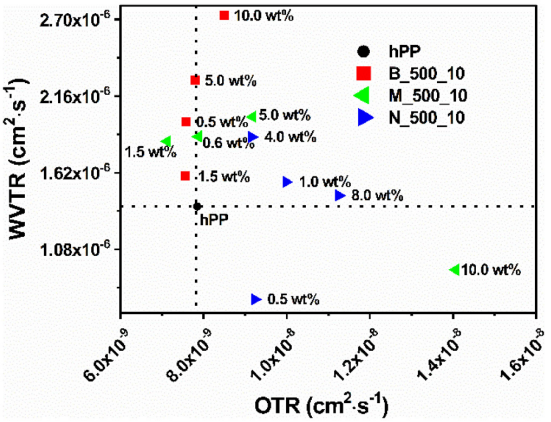

Figure 9. Correlation between WVTR and OTR for hPP and composites.

agents, promoting crystallite formation and modifying the structural properties of the composite[10,17,25]. However, at higher filler concentrations, interfacial defects may form, leading to increased permeability. For example, composites containing organophilic clay exhibited a 50% reduction in water vapor permeability compared to the PP matrix, while oxygen permeability experienced a slight increase[31].

The incorporation of $CaCO_3$ into PP significantly enhanced both thermal and transport properties, in agreement with previous reports. The composite containing 4.0 wt% $CaCO_3$ exhibited an HDT increase of up to 12 °C, consistent with Al-Samhan et al.[40], who attributed this improvement to the nucleating effect of the nanoparticles. Similarly, the highest crystallinity observed in the composite with 1.2 wt% corroborates the findings of Chafidz[41], highlighting the pronounced nucleation effect at low nanoparticle concentrations. Regarding barrier properties, the nanocomposite with 0.5 wt% $CaCO_3$ reduced oxygen permeability by 52%, in agreement with Al-Attar and Al-Samhan[42] who demonstrated that $CaCO_3$ particles act as effective diffusion barriers. Slight reductions in flammability observed for both nanocomposites and microcomposites align with Subasinghe et al.[43], who attributed to the formation of protective char layers—a residual carbon layer formed during combustion that acts as a physical barrier, reducing heat and oxygen transfer to the underlying material and slowing flame propagation. Overall, the produced nanocomposites outperformed microparticle-filled composites in enhancing thermal and transport properties. However, these improvements are not solely determined by particle size; they are also influenced by compatibilization and filler content, as emphasized by Fuad et al.[44]. These findings collectively demonstrate that carefully optimized nanocomposites can provide superior performance compared to conventional microparticle systems.

4. Conclusion

This study evaluated the thermal and transport properties of PP/$CaCO_3$ composites containing micro- and nanoparticles, processed at 500 rpm screw speed and 10 kg/h feed rate. The nanocomposite with 4.0 wt% $CaCO_3$ showed an HDT increase of up to 12 °C compared to neat PP, and the highest crystallinity was found in the composite with 1.2 wt%. Although the addition of mineral fillers reduced the OOT more noticeably in nanocomposites, it may indicate lower oxidative stability. Slight reductions in flammability were observed for the nanocomposite with 0.5 wt% and the microcomposite with 5.0 wt%. In terms of barrier properties, the nanocomposite with 0.5 wt% reduced oxygen permeability by 52%, though it did not present the best overall performance. In general, nanofillers improved thermal and transport properties more effectively than microparticles. However, these improvements are not solely dependent on particle size, but also on factors such as compatibilization and filler content. Further studies are needed to better understand these relationships

5. Author's Contribution

- **Conceptualization** – Juliano Martins Barbosa; Renato Meneghetti Peres; Bruno Milton Oliveira Silva; Ricardo Jorge Espanhol Andrade; Hélio Ribeiro.
- **Data curation** – Juliano Martins Barbosa; Hélio Ribeiro.
- **Formal analysis** – Juliano Martins Barbosa; Renato Meneghetti Peres; Bruno Milton Oliveira Silva; Ricardo Jorge Espanhol Andrade; Hélio Ribeiro.
- **Funding acquisition** - Juliano Martins Barbosa; Hélio Ribeiro.
- **Investigation** – Juliano Martins Barbosa; Hélio Ribeiro.
- **Methodology** – Juliano Martins Barbosa; Hélio Ribeiro.
- **Project administration** – Juliano Martins Barbosa; Hélio Ribeiro.
- **Resources** – Juliano Martins Barbosa; Renato Meneghetti Peres; Bruno Milton Oliveira Silva; Hélio Ribeiro.
- **Software** – N/A.
- **Supervision** – Juliano Martins Barbosa; Hélio Ribeiro.
- **Validation** – Juliano Martins Barbosa; Renato Meneghetti Peres; Bruno Milton Oliveira Silva; Ricardo Jorge Espanhol Andrade; Hélio Ribeiro.
- **Visualization** – Juliano Martins Barbosa; Renato Meneghetti Peres; Bruno Milton Oliveira Silva; Ricardo Jorge Espanhol Andrade; Hélio Ribeiro.
- **Writing – original draft** – Juliano Martins Barbosa; Hélio Ribeiro.
- **Writing – review & editing** – Juliano Martins Barbosa; Renato Meneghetti Peres; Bruno Milton Oliveira Silva; Ricardo Jorge Espanhol Andrade; Hélio Ribeiro.

6. Acknowledgements

This study received partial funding from the Coordenação de Aperfeiçoamento de Pessoal de Nível Superior - Brasil (CAPES) - Conselho Nacional de Desenvolvimento Científico e Tecnológico (CNPq, Project No. 305109/2022-7 and 303139/2024-2), Mackenzie Research Fund (Mackpesquisa, Project No. 231021, 0012510), and (Project No. 231015-0012510/002). Fundação de amparo à pesquisa do estado de São Paulo (FAPESP, Project No. 2023/08110-1. The authors extend their gratitude to the Materials Engineering Department (DEMa) of Federal University of São Carlos (UFSCar), as well as ZwickRoell and Netzsch - Analyzing and Testing for their invaluable technical support and collaboration in supplying the equipment utilized in this study and Cromex S/A, for raw material donation.

7. References

1. Rabelo, M. (2000). *Aditivação de polímeros*. São Paulo: Artliber Editora.
2. Wypych, G. (1999). *Handbook of fillers.* New York: Plastics Design Library.
3. Rodolfo, A., Nunes, L. R., & Ormanji, W. (2006). *Tecnologia do PVC.* São Paulo: ProEditores Associados.
4. Mai, Y. W., & Yu, Z.-Z. (Eds.). (2006). *Polymer nanocomposites*. Cambridge: Woodhead Publishing.
5. Barbosa, J. M. (2011). *Estudo das propriedades mecânicas, térmicas e de transporte do compósito com carbonato de cálcio nano e microparticulado em polipropileno* (Master's dissertation). Universidade Federal de São Carlos, São Carlos. Retrieved in 2025, July 5, from https://repositorio.ufscar.br/handle/ufscar/15929

6. Ribeiro, H., Silva, W. M., Neves, J. C., Calado, H. D. R., Paniago, R., Seara, L. M., Camarano, D. M., & Silva, G. G. (2015). Multifunctional nanocomposites based on tetraethylenepentamine-modified graphene oxide/epoxy. *Polymer Testing*, *43*, 182-192. https://doi.org/10.1016/j.polymertesting.2015.03.010.
7. Silva, B. M. O., Fernandes, N. M. M., Barbosa, J. M., Pinto, G. M., Benega, M. A. G., Taha-Tijerina, J. J., Andrade, R. J. E., & Ribeiro, H. (2024). Thermomechanical properties of multifunctional polymer hybrid nanocomposites based on carbon nanotubes and nanosilica. *Journal of Applied Polymer Science*, *141*(41), e56054. https://doi.org/10.1002/app.56054.
8. Móczó, J., & Pukánszky, B. (2019). *Particulate filled polypropylene: structure and properties.* In J. Karger-Kocsis, & T. Bárány (Eds.), *Structure an polypropylene handbook: morphology, blends and composites* (pp. 357-417). Cham: Springer. https://doi.org/10.1007/978-3-030-12903-3_7.
9. Barbosa, J. M., Beatrice, C. A. G., & Pessan, L. A. (2022). Influence of carbon black trimodal mixture on LDPE films properties: Part1 – DOE. *Polímeros: Ciência e Tecnologia*, *32*(3), e2022029. https://doi.org/10.1590/0104-1428.20220039.
10. Barbosa, J. M., Beatrice, C. A. G., & Pessan, L. A. (2022). Influence of carbon black trimodal mixture on LDPE films properties: Part2 – SME. *Polímeros: Ciência e Tecnologia*, vol. *32*, no. 3, e2022030. https://doi.org/10.1590/0104-1428.20220053.
11. Yang, K., Yang, Q., Li, G., Sun, Y., & Feng, D. (2006). Morphology and mechanical properties of polypropylene/calcium carbonate nanocomposites. *Materials Letters*, *60*(7), 805-809. https://doi.org/10.1016/j.matlet.2005.10.020.
12. Huang, Z., Lin, Z., Cai, Z., & Mai, K. (2004). Physical and mechanical properties of nano-CaCO3/PP composites modified with acrylic acid. *Plastics, Rubber and Composites*, *33*(8), 343-352. https://doi.org/10.1179/174328904X22314.
13. Barbosa, J. M. (2021). *Influência da incorporação de negro de fumo e carbonato de cálcio micro e nanoparticulado nas propriedades reológicas, colorimétricas e mecânicas de filmes de polietileno de baixa densidade* (Doctoral thesis). Universidade Federal de São Carlos, São Carlos. Retrieved in 2025, July 5, from https://repositorio.ufscar.br/handle/20.500.14289/16924
14. Demjén, Z., Pukánszky, B., & Nagy, J. (1998). Evaluation of interfacial interaction in polypropylene/surface treated $CaCO_3$ composites. *Composites. Part A, Applied Science and Manufacturing*, *29*(3), 323-329. https://doi.org/10.1016/S1359-835X(97)00032-8.
15. Fischer, H. (2003). Polymer nanocomposite: from fundamental research to specific applications. *Materials Science and Engineering C*, *23*(6-8), 763-772. https://doi.org/10.1016/j.msec.2003.09.148.
16. Jiang, L., Lam, Y. C., Tam, K. C., Chua, T. H., Sim, G. W., & Ang, L. S. (2005). Strengthening acrylonitrile-butadiene-styrene (ABS) with nano-sized and micron-sized calcium carbonate. *Polymer*, *46*(1), 243-252. https://doi.org/10.1016/j.polymer.2004.11.001.
17. Sakahara, R., Lima, A., & Wang, S. H. (2014). Influence of the beta crystalline phase fraction on the mechanical behavior of polypropylene/calcium carbonate/polypropylene-graft-maleic anhydride composites. *Polímeros: Ciência e Tecnologia*, *24*(5), 554-560. https://doi.org/10.1590/0104-1428.1692.
18. Avella, M., Cosco, S., Di Lorenzo, M. L., Di Pace, E., Errico, M. E., & Gentile, G. (2006). Nucleation activity of nanosized $CaCO_3$ on crystallization of isotactic PP: dependence on crystal modification, particle shape, and coating. *European Polymer Journal*, *42*(6), 1548-1557. https://doi.org/10.1016/j.eurpolymj.2006.01.009.
19. Zhang, Q.-X., Yu, Z.-Z., Xie, X.-L., & Mai, Y.-W. (2004). Crystallization and impact energy of polypropylene/$CaCO_3$ nanocomposites with nonionic modifier. *Polymer*, *45*(17), 5985-5994. https://doi.org/10.1016/j.polymer.2004.06.044.
20. Barbosa, J. M., Pacheco, C. V., Szilagyi, G., Oliveira, P. C. M., Peres, R. M., & Ribeiro, H. (2022). *Mechanical properties of polypropylene/calcium carbonate micro and nanocomposites.* In *17th Brazilian Polymer Congress (CBPol)*, Joinville, Brazil.
21. Barbosa, J. M., Pacheco, C. V., Szilágyi, G., Oliveira, P. C., Peres, R. M., & Ribeiro, H. (2024). Micro and nanoparticulate PP/$CaCO_3$ composites mechanical, thermal and transport properties - DOE. *Polímeros: Ciência e Tecnologia*, *35*(1), e20250003. https://doi.org/10.1590/0104-1428.20240071.
22. Alves, T. S., Barbosa, R., Carvalho, L. H., & Canedo, E. L. (2014). Inflamabilidade de nanocompósitos de polipropileno/argila organofílica. *Polímeros: Ciência e Tecnologia*, *24*(3), 334-340. https://doi.org/10.4322/polimeros.2014.030.
23. Alberton, J. (2008). *Preparação e caracterização de compósitos de polipropileno, carbonato de cálcio e poli(etileno-co-acetato de vinila) utilizados na produção de chapas termoplásticas* (Master's dissertation). Universidade Federal de Santa Catarina, Florianópolis. Retrieved in 2025, July 5, from https://repositorio.ufsc.br/handle/123456789/91059
24. Hadi, N. J., Saad, N. A., & Mohamed, D. J. (2016). Thermal behavior of calcium carbonate and zinc oxide nanoparticles filled polypropylene by melt compounding. *Research Journal of Applied Sciences, Engineering and Technology*, *13*(4), 265-272. https://doi.org/10.19026/rjaset.13.2941.
25. Loste, J., Lopez-Cuesta, J.-M., Billon, L., Garay, H., & Save, M. (2019). Transparent polymer nanocomposites: an overview on their synthesis and advanced properties. *Progress in Polymer Science*, *89*, 133-158. https://doi.org/10.1016/j.progpolymsci.2018.10.003.
26. Al-Samhan, M., & Al-Attar, F. (2022). Comparative analysis of the mechanical, thermal, and barrier properties of polypropylene incorporated with $CaCO_3$ and nano $CaCO_3$. *Surfaces and Interfaces*, *31*, 102055. https://doi.org/10.1016/j.surfin.2022.102055.
27. Kamal, M., Sharma, C. S., Upadhyaya, P., Verma, V., Pandey, K. N., Kumar, V., & Agrawal, D. D. (2012). Calcium carbonate ($CaCO_3$) nanoparticle filled polypropylene: effect of particle surface treatment on mechanical, thermal, and morphological performance of composites. *Journal of Applied Polymer Science*, *124*(4), 2649-2656. https://doi.org/10.1002/app.35319.
28. American Society for Testing and Materials – ASTM. (2006). *ASTM D648-06: standard test method for deflection temperature of plastics under flexural load in the edgewise position.* West Conshohocken: ASTM. https://doi.org/10.1520/D0648-18.
29. American Society for Testing and Materials – ASTM. (2008). *ASTM E2009-08: standard test method for oxidation onset temperature of hydrocarbons by differential scanning calorimetry.* West Conshohocken: ASTM. https://doi.org/10.1520/E2009-08.
30. American National Standards Institute – ANSI. (2024). *UL 94: tests for flammability of plastics materials for parts and devices and appliances.* Washington, D.C.: ANSI.
31. Morelli, F. C. (2009). *Nanocompósito de PP/PP-g-AM/argila organofílica: processamento, propriedades mecânicas, termo-mecânicas e de permeação de gás* (Master's dissertation). Universidade Federal de São Carlos, São Carlos.
32. American Society for Testing and Materials – ASTM. (2024). *ASTM E96/E96M-24a: standard test methods for gravimetric determination of water vapor transmission rate of materials.* West Conshohocken: ASTM. https://doi.org/10.1520/E0096_E0096M-24A.
33. Atkins, P. W. (1990). *Physical chemistry.* Oxford: Oxford University Press.

34. American Society for Testing and Materials – ASTM. (2024). *ASTM D3985: standard test method for oxygen gas transmission rate through plastic film and sheeting using a coulometric sensor.* West Conshohocken: ASTM. https://doi.org/10.1520/D3985-24.
35. Rothon, R. N. (Ed.). (2003). *Particulate filled polymer composites.* Shrewsbury: Rapra Technology.
36. Chan, C.-M., Wu, J., Li, J.-X., & Cheung, Y.-K. (2002). Polypropylene/calcium carbonate nanocomposite. *Polymer*, *43*(10), 2981-2992. https://doi.org/10.1016/S0032-3861(02)00120-9.
37. Eiras, D. (2009). *Tenacificação de polipropileno com nanopartículas de carbonato de cálcio* (Master's dissertation). Universidade Federal de São Carlos, São Carlos.
38. Bertini, F., Canetti, M., Audisio, G., Costa, G., & Falqui, L. (2006). Characterization and thermal degradation of polypropylene-montmorillonite nanocomposites. *Polymer Degradation & Stability*, *91*(3), 600-605. https://doi.org/10.1016/j.polymdegradstab.2005.02.027.
39. Fitaroni, L. B., Lima, J. A., Cruz, S. A., & Waldman, W. R. (2015). Thermal stability of PP–montmorillonite clay nanocomposites: limitation of the TA. *Polymer Degradation & Stability*, *111*, 102-108. https://doi.org/10.1016/j.polymdegradstab.2014.10.016.
40. Al-Samhan, M., Al-Attar, F., Al-Fadhli, J., & Al-Shamali, M. (2021). The influence of nano-$CaCO_3$ on nucleation and interface of PP nanocomposite: matrix processability and impact resistance. *Polymers*, *13*(9), 1389. https://doi.org/10.3390/polym13091389. PMid:33922878.
41. Chafidz, A. (2022). Effect of nano-$CaCO_3$ loadings and re-processing on the melting properties of polypropylene/calcium carbonate nanocomposites. *Materials Science Forum*, *1067*, 73-78. https://doi.org/10.4028/p-2u9f04.
42. Al-Attar, F., & Al-Samhan, M. (2022). Nano $CaCO_3$ incorporation with polypropylene to reduce film water vapor permeability for packaging application. *Asian Journal of Scientific Research*, *13*(4), 275-283. https://doi.org/10.3923/ajsr.2020.275.283.
43. Subasinghe, A., Das, R., & Bhattacharyya, D. (2016). Study of thermal, flammability and mechanical properties of intumescent flame-retardant PP/kenaf nanocomposites. *International Journal of Smart and Nano Materials*, *7*(3), 202-220. https://doi.org/10.1080/19475411.2016.1239315.
44. Fuad, M. Y. A., Hanim, H., Zarina, R., Ishak, Z. A. M., & Hassan, A. (2010). Polypropylene/calcium carbonate nanocomposites: effects of processing techniques and maleated polypropylene compatibilizer. *Express Polymer Letters*, *4*(10), 611-620. https://doi.org/10.3144/expresspolymlett.2010.76.

Received: Jul. 05, 2025
Revised: Oct. 04, 2025
Accepted: Nov. 14, 2025

Editor-in-Chief: *Sebastião V. Canevarolo*